EUROPEAN ORGANIZATION FOR NUCLEAR RESEARCH

CERN–PPE/96-61

6 May 1996

Search for anomalous production of single photons at $\sqrt{s}$ =130 and 136 GeV

DELPHI Collaboration

Abstract

This letter reports the results of the measurement of single photon production in the reaction $e^+e^- \to \gamma +$ invisible particles at centre-of-mass energies $\sqrt{s}$ = 130 and 136 GeV and an integrated luminosity of 5.83 pb^{-1}, collected with the DELPHI detector at LEP. The signal is compatible with the prediction of the Standard Model for the process $e^+e^- \to \nu\bar{\nu}\gamma$, and the number of neutrino families has been determined to be $N_\nu = 3.1 \pm 0.6$. Limits have been derived on anomalous neutral gauge boson couplings and on compositeness in the framework of a specific model.

(To be submitted to Physics Letters B)

W.Adam[50], T.Adye[37], E.Agasi[31], I.Ajinenko[42], R.Aleksan[39], G.D.Alekseev[16], R.Alemany[49], P.P.Allport[22], S.Almehed[24], U.Amaldi[9], S.Amato[47], A.Andreazza[28], M.L.Andrieux[14], P.Antilogus[9], W-D.Apel[17], Y.Arnoud[39], B.Åsman[44], J-E.Augustin[25], A.Augustinus[9], P.Baillon[9], P.Bambade[19], F.Barao[21], R.Barate[14], M.Barbi[47], G.Barbiellini[46], D.Y.Bardin[16], A.Baroncelli[40], O.Barring[24], J.A.Barrio[26], W.Bartl[50], M.J.Bates[37], M.Battaglia[15], M.Baubillier[23], J.Baudot[39], K-H.Becks[52], M.Begalli[6], P.Beilliere[8], Yu.Belokopytov[9,53], K.Belous[42], A.C.Benvenuti[5], M.Berggren[47], D.Bertini[25], D.Bertrand[2], F.Bianchi[45], M.Bigi[45], M.S.Bilenky[16], P.Billoir[23], D.Bloch[10], M.Blume[52], T.Bolognese[39], M.Bonesini[28], W.Bonivento[28], P.S.L.Booth[22], C.Bosio[40], O.Botner[48], E.Boudinov[31], B.Bouquet[19], C.Bourdarios[9], T.J.V.Bowcock[22], M.Bozzo[13], P.Branchini[40], K.D.Brand[36], T.Brenke[52], R.A.Brenner[15], C.Bricman[2], R.C.A.Brown[9], P.Bruckman[18], J-M.Brunet[8], L.Bugge[33], T.Buran[33], T.Burgsmueller[52], P.Buschmann[52], A.Buys[9], S.Cabrera[49], M.Caccia[28], M.Calvi[28], A.J.Camacho Rozas[41], T.Camporesi[9], V.Canale[38], M.Canepa[13], K.Cankocak[44], F.Cao[2], F.Carena[9], L.Carroll[22], C.Caso[13], M.V.Castillo Gimenez[49], A.Cattai[9], F.R.Cavallo[5], V.Chabaud[9], Ph.Charpentier[9], L.Chaussard[25], J.Chauveau[23], P.Checchia[36], G.A.Chelkov[16], M.Chen[2], R.Chierici[45], P.Chliapnikov[42], P.Chochula[7], V.Chorowicz[9], V.Cindro[43], P.Collins[9], J.L.Contreras[19], R.Contri[13], E.Cortina[49], G.Cosme[19], F.Cossutti[46], H.B.Crawley[1], D.Crennell[37], G.Crosetti[13], J.Cuevas Maestro[34], S.Czellar[15], E.Dahl-Jensen[29], J.Dahm[52], B.Dalmagne[19], M.Dam[29], G.Damgaard[29], P.D.Dauncey[37], M.Davenport[9], W.Da Silva[23], C.Defoix[8], A.Deghorain[2], G.Della Ricca[46], P.Delpierre[27], N.Demaria[35], A.De Angelis[9], W.De Boer[17], S.De Brabandere[2], C.De Clercq[2], C.De La Vaissiere[23], B.De Lotto[46], A.De Min[36], L.De Paula[47], C.De Saint-Jean[39], H.Dijkstra[9], L.Di Ciaccio[38], F.Djama[10], J.Dolbeau[8], M.Donszelmann[9], K.Doroba[51], M.Dracos[10], J.Drees[52], K.-A.Drees[52], M.Dris[32], J-D.Durand[25], D.Edsall[1], R.Ehret[17], G.Eigen[4], T.Ekelof[48], G.Ekspong[44], M.Elsing[52], J-P.Engel[10], B.Erzen[43], M.Espirito Santo[21], E.Falk[24], D.Fassouliotis[32], M.Feindt[9], A.Fenyuk[42], A.Ferrer[49], S.Fichet[23], T.A.Filippas[32], A.Firestone[1], P.-A.Fischer[10], H.Foeth[9], E.Fokitis[32], F.Fontanelli[13], F.Formenti[9], B.Franek[37], P.Frenkiel[8], D.C.Fries[17], A.G.Frodesen[4], R.Fruhwirth[50], F.Fulda-Quenzer[19], J.Fuster[49], A.Galloni[22], D.Gamba[45], M.Gandelman[6], C.Garcia[49], J.Garcia[41], C.Gaspar[9], U.Gasparini[36], Ph.Gavillet[9], E.N.Gazis[32], D.Gele[10], J-P.Gerber[10], M.Gibbs[22], R.Gokieli[51], B.Golob[43], G.Gopal[37], L.Gorn[1], M.Gorski[51], Yu.Gouz[45,53], V.Gracco[13], E.Graziani[40], G.Grosdidier[19], K.Grzelak[51], S.Gumenyuk[28,53], P.Gunnarsson[44], M.Gunther[48], J.Guy[37], F.Hahn[9], S.Hahn[52], Z.Hajduk[18], A.Hallgren[48], K.Hamacher[52], W.Hao[31], F.J.Harris[35], V.Hedberg[24], R.Henriques[21], J.J.Hernandez[49], P.Herquet[2], H.Herr[9], T.L.Hessing[35], E.Higon[49], H.J.Hilke[9], T.S.Hill[1], S-O.Holmgren[44], P.J.Holt[35], D.Holthuizen[31], S.Hoorelbeke[2], M.Houlden[22], J.Hrubec[50], K.Huet[2], K.Hultqvist[44], J.N.Jackson[22], R.Jacobsson[44], P.Jalocha[18], R.Janik[7], Ch.Jarlskog[24], G.Jarlskog[24], P.Jarry[39], B.Jean-Marie[19], E.K.Johansson[44], L.Jonsson[24], P.Jonsson[24], C.Joram[9], P.Juillot[10], M.Kaiser[17], F.Kapusta[23], K.Karafasoulis[11], M.Karlsson[44], E.Karvelas[11], S.Katsanevas[3], E.C.Katsoufis[32], R.Keranen[4], Yu.Khokhlov[42], B.A.Khomenko[16], N.N.Khovanski[16], B.King[22], N.J.Kjaer[29], H.Klein[9], A.Klovning[4], P.Kluit[31], B.Koene[31], P.Kokkinias[11], M.Koratzinos[9], K.Korcyl[18], V.Kostioukhine[42], C.Kourkoumelis[3], O.Kouznetsov[13,16], P.-H.Kramer[52], M.Krammer[50], C.Kreuter[17], I.Kronkvist[24], Z.Krumstein[16], W.Krupinski[18], P.Kubinec[7], W.Kucewicz[18], K.Kurvinen[15], C.Lacasta[49], I.Laktineh[25], S.Lamblot[23], J.W.Lamsa[1], L.Lanceri[46], D.W.Lane[1], P.Langefeld[52], V.Lapin[42], I.Last[22], J-P.Laugier[39], R.Lauhakangas[15], G.Leder[50], F.Ledroit[14], V.Lefebure[2], C.K.Legan[1], R.Leitner[30], Y.Lemoigne[39], J.Lemonne[2], G.Lenzen[52], V.Lepeltier[19], T.Lesiak[18], J.Libby[35], D.Liko[50], R.Lindner[52], A.Lipniacka[36], I.Lippi[36], B.Loerstad[24], J.G.Loken[35], J.M.Lopez[41], D.Loukas[11], P.Lutz[39], L.Lyons[35], J.MacNaughton[50], G.Maehlum[17], A.Maio[21], V.Malychev[16], J.Marco[41], R.Marco[41], B.Marechal[47], M.Margoni[36], J-C.Marin[9], C.Mariotti[40], A.Markou[11], T.Maron[52], C.Martinez-Rivero[41], F.Martinez-Vidal[49], S.Marti i Garcia[49], F.Matorras[41], C.Matteuzzi[9], G.Matthiae[38], M.Mazzucato[36], M.Mc Cubbin[9], R.Mc Kay[1], R.Mc Nulty[22], J.Medbo[48], M.Merk[31], C.Meroni[28], S.Meyer[17], W.T.Meyer[1], A.Miagkov[42], M.Michelotto[36], E.Migliore[45], L.Mirabito[25], W.A.Mitaroff[50], U.Mjoernmark[24], T.Moa[44], R.Moeller[29], K.Moenig[9], M.R.Monge[13], P.Morettini[13], H.Mueller[17], L.M.Mundim[6], W.J.Murray[37], B.Muryn[18], G.Myatt[35], F.Naraghi[14], F.L.Navarria[5], S.Navas[49], K.Nawrocki[51], P.Negri[28], S.Nemecek[12], W.Neumann[52], N.Neumeister[50], R.Nicolaidou[3], B.S.Nielsen[29], M.Nieuwenhuizen[31], V.Nikolaenko[10], P.Niss[44], A.Nomerotski[36], A.Normand[35], M.Novak[12], W.Oberschulte-Beckmann[17], V.Obraztsov[42], A.G.Olshevski[16], A.Onofre[21], R.Orava[15], K.Osterberg[15], A.Ouraou[39], P.Paganini[19], M.Paganoni[9], P.Pages[10], H.Palka[18], Th.D.Papadopoulou[32], K.Papageorgiou[11], L.Pape[9], C.Parkes[35], F.Parodi[13], A.Passeri[40], M.Pegoraro[36], L.Peralta[21], H.Pernegger[50], M.Pernicka[50], A.Perrotta[5], C.Petridou[46], A.Petrolini[13], M.Petrovyck[28,53], H.T.Phillips[37], G.Piana[13], F.Pierre[39], M.Pimenta[21], M.Pindo[28], S.Plaszczynski[19], O.Podobrin[17], M.E.Pol[6], G.Polok[18], P.Poropat[46], V.Pozdniakov[16], M.Prest[46], P.Privitera[38], N.Pukhaeva[16], A.Pullia[28], D.Radojicic[35], S.Ragazzi[28], H.Rahmani[32], J.Rames[12], P.N.Ratoff[20], A.L.Read[33], M.Reale[52], P.Rebecchi[19], N.G.Redaelli[28], M.Regler[50], D.Reid[9], P.B.Renton[35], L.K.Resvanis[3], F.Richard[19], J.Richardson[22], J.Ridky[12], G.Rinaudo[45], I.Ripp[39], A.Romero[45], I.Roncagliolo[13], P.Ronchese[36], L.Roos[14], E.I.Rosenberg[1], E.Rosso[9], P.Roudeau[19], T.Rovelli[5], W.Ruckstuhl[31], V.Ruhlmann-Kleider[39], A.Ruiz[41], K.Rybicki[18], H.Saarikko[15], Y.Sacquin[39], A.Sadovsky[16], O.Sahr[14], G.Sajot[14], J.Salt[49], J.Sanchez[26], M.Sannino[13], M.Schimmelpfennig[17], H.Schneider[17], U.Schwickerath[17], M.A.E.Schyns[52], G.Sciolla[45], F.Scuri[46], P.Seager[20], Y.Sedykh[16], A.M.Segar[35], A.Seitz[17], R.Sekulin[37], L.Serbelloni[38], R.C.Shellard[6], I.Siccama[31], P.Siegrist[39], S.Simonetti[39], F.Simonetto[36], A.N.Sisakian[16], B.Sitar[7], T.B.Skaali[33], G.Smadja[25], N.Smirnov[42], O.Smirnova[24], G.R.Smith[37], R.Sosnowski[51], D.Souza-Santos[6], T.Spassov[21], E.Spiriti[40], P.Sponholz[52], S.Squarcia[13], C.Stanescu[40], S.Stapnes[33], I.Stavitski[36], K.Stevenson[35], F.Stichelbaut[9], A.Stocchi[19], J.Strauss[50], R.Strub[10], B.Stugu[4], M.Szczekowski[51], M.Szeptycka[51], T.Tabarelli[28], J.P.Tavernet[23],

O.Tchikilev[42], J.Thomas[35], A.Tilquin[27], J.Timmermans[31], L.G.Tkatchev[16], T.Todorov[10], S.Todorova[10], D.Z.Toet[31], A.Tomaradze[2], B.Tome[21], A.Tonazzo[28], L.Tortora[40], G.Transtromer[24], D.Treille[9], W.Trischuk[9], G.Tristram[8], A.Trombini[19], C.Troncon[28], A.Tsirou[9], M-L.Turluer[39], I.A.Tyapkin[16], M.Tyndel[37], S.Tzamarias[22], B.Ueberschaer[52], O.Ullaland[9], V.Uvarov[42], G.Valenti[5], E.Vallazza[9], G.W.Van Apeldoorn[31], P.Van Dam[31], W.K.Van Doninck[2], J.Van Eldik[31], N.Vassilopoulos[35], G.Vegni[28], L.Ventura[36], W.Venus[37], F.Verbeure[2], M.Verlato[36], L.S.Vertogradov[16], D.Vilanova[39], P.Vincent[25], L.Vitale[46], E.Vlasov[42], A.S.Vodopyanov[16], V.Vrba[12], H.Wahlen[52], C.Walck[44], M.Weierstall[52], P.Weilhammer[9], C.Weiser[17], A.M.Wetherell[9], D.Wicke[52], J.H.Wickens[2], M.Wielers[17], G.R.Wilkinson[35], W.S.C.Williams[35], M.Winter[10], M.Witek[18], K.Woschnagg[48], K.Yip[35], O.Yushchenko[42], F.Zach[25], A.Zaitsev[42], A.Zalewska[9], P.Zalewski[51], D.Zavrtanik[43], E.Zevgolatakos[11], N.I.Zimin[16], M.Zito[39], D.Zontar[43], G.C.Zucchelli[44], G.Zumerle[36]

[1] Ames Laboratory and Department of Physics, Iowa State University, Ames IA 50011, USA
[2] Physics Department, Univ. Instelling Antwerpen, Universiteitsplein 1, B-2610 Wilrijk, Belgium
and IIHE, ULB-VUB, Pleinlaan 2, B-1050 Brussels, Belgium
and Faculté des Sciences, Univ. de l'Etat Mons, Av. Maistriau 19, B-7000 Mons, Belgium
[3] Physics Laboratory, University of Athens, Solonos Str. 104, GR-10680 Athens, Greece
[4] Department of Physics, University of Bergen, Allégaten 55, N-5007 Bergen, Norway
[5] Dipartimento di Fisica, Università di Bologna and INFN, Via Irnerio 46, I-40126 Bologna, Italy
[6] Centro Brasileiro de Pesquisas Físicas, rua Xavier Sigaud 150, RJ-22290 Rio de Janeiro, Brazil
and Depto. de Física, Pont. Univ. Católica, C.P. 38071 RJ-22453 Rio de Janeiro, Brazil
and Inst. de Física, Univ. Estadual do Rio de Janeiro, rua São Francisco Xavier 524, Rio de Janeiro, Brazil
[7] Comenius University, Faculty of Mathematics and Physics, Mlynska Dolina, SK-84215 Bratislava, Slovakia
[8] Collège de France, Lab. de Physique Corpusculaire, IN2P3-CNRS, F-75231 Paris Cedex 05, France
[9] CERN, CH-1211 Geneva 23, Switzerland
[10] Centre de Recherche Nucléaire, IN2P3 - CNRS/ULP - BP20, F-67037 Strasbourg Cedex, France
[11] Institute of Nuclear Physics, N.C.S.R. Demokritos, P.O. Box 60228, GR-15310 Athens, Greece
[12] FZU, Inst. of Physics of the C.A.S. High Energy Physics Division, Na Slovance 2, 180 40, Praha 8, Czech Republic
[13] Dipartimento di Fisica, Università di Genova and INFN, Via Dodecaneso 33, I-16146 Genova, Italy
[14] Institut des Sciences Nucléaires, IN2P3-CNRS, Université de Grenoble 1, F-38026 Grenoble Cedex, France
[15] Research Institute for High Energy Physics, SEFT, P.O. Box 9, FIN-00014 Helsinki, Finland
[16] Joint Institute for Nuclear Research, Dubna, Head Post Office, P.O. Box 79, 101 000 Moscow, Russian Federation
[17] Institut für Experimentelle Kernphysik, Universität Karlsruhe, Postfach 6980, D-76128 Karlsruhe, Germany
[18] Institute of Nuclear Physics and University of Mining and Metalurgy, Ul. Kawiory 26a, PL-30055 Krakow, Poland
[19] Université de Paris-Sud, Lab. de l'Accélérateur Linéaire, IN2P3-CNRS, Bât. 200, F-91405 Orsay Cedex, France
[20] School of Physics and Chemistry, University of Lancaster, Lancaster LA1 4YB, UK
[21] LIP, IST, FCUL - Av. Elias Garcia, 14-1°, P-1000 Lisboa Codex, Portugal
[22] Department of Physics, University of Liverpool, P.O. Box 147, Liverpool L69 3BX, UK
[23] LPNHE, IN2P3-CNRS, Universités Paris VI et VII, Tour 33 (RdC), 4 place Jussieu, F-75252 Paris Cedex 05, France
[24] Department of Physics, University of Lund, Sölvegatan 14, S-22363 Lund, Sweden
[25] Université Claude Bernard de Lyon, IPNL, IN2P3-CNRS, F-69622 Villeurbanne Cedex, France
[26] Universidad Complutense, Avda. Complutense s/n, E-28040 Madrid, Spain
[27] Univ. d'Aix - Marseille II - CPP, IN2P3-CNRS, F-13288 Marseille Cedex 09, France
[28] Dipartimento di Fisica, Università di Milano and INFN, Via Celoria 16, I-20133 Milan, Italy
[29] Niels Bohr Institute, Blegdamsvej 17, DK-2100 Copenhagen 0, Denmark
[30] NC, Nuclear Centre of MFF, Charles University, Areal MFF, V Holesovickach 2, 180 00, Praha 8, Czech Republic
[31] NIKHEF-H, Postbus 41882, NL-1009 DB Amsterdam, The Netherlands
[32] National Technical University, Physics Department, Zografou Campus, GR-15773 Athens, Greece
[33] Physics Department, University of Oslo, Blindern, N-1000 Oslo 3, Norway
[34] Dpto. Fisica, Univ. Oviedo, C/P. Pérez Casas, S/N-33006 Oviedo, Spain
[35] Department of Physics, University of Oxford, Keble Road, Oxford OX1 3RH, UK
[36] Dipartimento di Fisica, Università di Padova and INFN, Via Marzolo 8, I-35131 Padua, Italy
[37] Rutherford Appleton Laboratory, Chilton, Didcot OX11 OQX, UK
[38] Dipartimento di Fisica, Università di Roma II and INFN, Tor Vergata, I-00173 Rome, Italy
[39] Centre d'Etudes de Saclay, DSM/DAPNIA, F-91191 Gif-sur-Yvette Cedex, France
[40] Istituto Superiore di Sanità, Ist. Naz. di Fisica Nucl. (INFN), Viale Regina Elena 299, I-00161 Rome, Italy
[41] Instituto de Fisica de Cantabria (CSIC-UC), Avda. los Castros, S/N-39006 Santander, Spain, (CICYT-AEN93-0832)
[42] Inst. for High Energy Physics, Serpukov P.O. Box 35, Protvino, (Moscow Region), Russian Federation
[43] J. Stefan Institute and Department of Physics, University of Ljubljana, Jamova 39, SI-61000 Ljubljana, Slovenia
[44] Fysikum, Stockholm University, Box 6730, S-113 85 Stockholm, Sweden
[45] Dipartimento di Fisica Sperimentale, Università di Torino and INFN, Via P. Giuria 1, I-10125 Turin, Italy
[46] Dipartimento di Fisica, Università di Trieste and INFN, Via A. Valerio 2, I-34127 Trieste, Italy
and Istituto di Fisica, Università di Udine, I-33100 Udine, Italy
[47] Univ. Federal do Rio de Janeiro, C.P. 68528 Cidade Univ., Ilha do Fundão BR-21945-970 Rio de Janeiro, Brazil
[48] Department of Radiation Sciences, University of Uppsala, P.O. Box 535, S-751 21 Uppsala, Sweden
[49] IFIC, Valencia-CSIC, and D.F.A.M.N., U. de Valencia, Avda. Dr. Moliner 50, E-46100 Burjassot (Valencia), Spain
[50] Institut für Hochenergiephysik, Österr. Akad. d. Wissensch., Nikolsdorfergasse 18, A-1050 Vienna, Austria
[51] Inst. Nuclear Studies and University of Warsaw, Ul. Hoza 69, PL-00681 Warsaw, Poland
[52] Fachbereich Physik, University of Wuppertal, Postfach 100 127, D-42097 Wuppertal 1, Germany
[53] On leave of absence from IHEP Serpukhov

1 Introduction

The process

$$e^+e^- \rightarrow \gamma + \text{invisible particles} \quad (1)$$

receives a contribution within the Standard Model (SM) from the radiative production of neutrino-antineutrino pairs. At the centre of mass energies studied in this letter, this production of a single photon is described by $s-$ and $t-$ channel diagrams involving the exchange of a Z and a $W^{\pm}$ respectively (the W contributing only to the production of electron-neutrino). The radiation of a photon from the exchanged W is also taken into account in a precise cross-section calculation of the above process [1].

A new generation of neutrinos or the radiative production of any other neutral weakly interacting or invisibly decaying particles would give an additional contribution to the cross-section for process (1). In this letter, after having measured with (1) the number of light neutrino generations (section 3.1), a search is made for triple gauge neutral boson couplings (section 3.2), for compositeness (section 3.3) and for heavy stable neutral particles (section 3.4). Theories of supersymmetry (SUSY) also predict [2] the existence of particles which would be produced in (1) [3], but with too small a cross-section in the energy range and collected luminosity studied in this letter.

2 Event selection

The general criteria for the selection of events are based on the electromagnetic calorimeters and the tracking system of the DELPHI detector [4].

Single photons are searched for in the barrel region, covered by the High density Projection Chamber (HPC) in the range $40^\circ < \theta < 140^\circ$, where θ is the polar angle with respect to the incoming electron direction, and in the forward region, covered by the Forward Electromagnetic Calorimeter (FEMC) in the ranges $8^\circ < \theta < 35^\circ$ and $145^\circ < \theta < 172^\circ$.

The HPC is a gas sampling calorimeter of total thickness of 17.5 radiation lengths (X_0), which samples each shower nine times longitudinally. It has an energy resolution $\sigma(E)/E = 0.32/\sqrt{E} \oplus 0.043$ (with E in GeV), where the symbol $\oplus$ means addition in quadrature.

The FEMC is a homogeneous calorimeter consisting of lead glass blocks with a depth of about 20 X_0, providing an energy resolution of $\sigma(E)/E = 0.12/\sqrt{E} \oplus 0.03 \oplus 0.11/E$ and a readout granularity of about 1° both in θ and in ϕ.

Events were selected for the present analysis if there were no charged particles detected in the main tracking device of DELPHI, the Time Projection Chamber (TPC), coming from the interaction point. The TPC covers the polar angle region $20^\circ < \theta < 160^\circ$. Events were also rejected if there were tracks in the forward region of the detector or in the TPC which did not come from the interaction region; this cut reduces the backgrounds from beam-gas interactions and cosmic rays.

In order to reduce the background from radiative Bhabha events, no energy deposit greater than 3 GeV was allowed in the Small angle TIle Calorimeter (STIC),which covers the very forward angular regions $1.7^\circ < \theta < 10.6^\circ$ and $169.4^\circ < \theta < 178.3^\circ$. STIC is the DELPHI luminosity monitor.

2.1 Shower Selection in the HPC

Some criteria were imposed in order to select showers produced by photons originating from the interaction point. They exploit the high granularity of the detector, which allows a detailed analysis of the shower development. Only showers having an energy, E_γ, greater than 2 GeV and the polar angle of the axis of the shower, θ_γ, in the angular region $45° < \theta_\gamma < 135°$ were considered (the shower axis considered here is the photon line of flight). They were selected as good electromagnetic showers if they started within the first 2.5 X_0 of the calorimeter, if they released energy in at least 3 of the 9 sampling rows, and if they had no more than one empty row before the end of the shower development. In order to reject α particles emitted from the radioactive lead, it was required that no row contains more than 90% of the shower energy. The polar angle of the shower axis had to be outside the range 88° to 92°, where the HPC has a dead region. The shower direction was required be consistent with the photon originating from the interaction point. The angle between the line of flight of the photon and the direction of the shower as measured inside the calorimeter was required to be less than 15°. The last criteria strongly suppress events induced by cosmic rays. The remaining cosmic ray contamination was rejected by the presence of aligned hits in the muon chambers, or in the hadron calorimeter or in the time of flight counters (19 events were found in this category).

In all, 20 events were retained, out of 39 preliminary candidates, after application of all the selection criteria.

2.2 Shower Selection in the FEMC

The projective structure of the FEMC and the small probability of a cosmic ray simulating a photon in the forward calorimeter made the selection of good quality showers in the forward regions simpler than in the barrel. The ranges in energy and angle were restricted to $E_\gamma > 10$ GeV and $12° < \theta_\gamma < 34°$ or $146° < \theta_\gamma < 168°$ respectively. The requirement that no charged particle is detected lowers the efficiency significantly in the forward region, because the ~ 2 X_0 of material in front of the calorimeter cause most of the photons to convert before reaching the FEMC. The photon energy was required to be less than 50 GeV in order to reject $e^+e^- \to \gamma\gamma$ events in which one of the final photons escaped detection.

A total of 17 candidates passed the selection criteria in the forward angular region.

2.3 Efficiencies

To measure the cross-section, the events were corrected for the trigger efficiency and for the identification efficiency.

The latter depends on the criteria applied to select a good electromagnetic shower. It was determined on the basis of a sample of Monte Carlo events passed through the complete simulation of the DELPHI detector. The generator used was from [1]. The efficiency was then determined as a function of E_γ and θ_γ.

In the case of the HPC selection, the identification efficiency depends on the photon energy, and ranges from $(42 \pm 2)\%$ for low energies, to $(73 \pm 1)\%$ for $E_\gamma > 10$ GeV. In the FEMC, the selection requirements retain $(40.0 \pm 1.5)\%$ of the photons. In both cases a loss of efficiency of about 2% due to noisy modules was taken into account.

Single photon events were triggered by requiring a hit in a cylindrical set of scintillators [5] located at the mean shower maximum in the HPC or by the standard photo-triode readout from the FEMC lead glass blocks. The trigger efficiency was measured with

radiative Bhabha and Compton events [5]. In the HPC it was found to be strongly dependent on the photon energy, up to $\sim$ 6 GeV. It varies from 10% to 60% from 2 to 6 GeV, and is $(60.0 \pm 2.5)\%$ for $E_\gamma > 6$ GeV. In the FEMC the trigger efficiency is $(97.0 \pm 0.1)\%$ for $E_\gamma > 10$ GeV.

2.4 Background

The main source of background is the QED process $e^+e^- \to \gamma e^+e^-$ where the two electrons escape undetected along the beam pipe. This process has a very high cross-section [6], decreasing rapidly when E_γ and the photon polar angle increase. This behaviour of the QED background was the reason for applying the $E_\gamma > 10$ GeV cut in the forward region.

The contamination from the QED process was calculated on the basis of [6] and found to be (3.7 ± 0.2) events in the forward region and (1.5 ± 0.2) events in the barrel. A critical parameter in the calculation is the cone around the beam axis where the electrons escape detection; this is determined by the lower edge of the STIC calorimeter, which on one side is defined with a precision better than $< 10^{-3}$ degrees by a tungsten mask (which also reduces the acceptance by 0.9 degree on this side), and on the opposite side is known with an accuracy of ~ 0.1 degrees.

For other backgrounds, such as beam gas, $\gamma\gamma$ collisions, $e^+e^- \to \gamma\gamma(\gamma)$, the computed contributions were found to be negligible.

3 Analysis of the single photon sample

The event selection procedure left 20 events in the barrel region (HPC) and 17 in the forward region (FEMC). The energy spectrum of the selected events is shown in figure 1.

After correcting for background and efficiencies, and using the integrated luminosity of 5.83 pb^{-1}, the two separate cross-sections measured within the acceptances are

$$\sigma(e^+e^- \to \gamma + \text{invisible particles}) = (7.9 \pm 1.9) \text{ pb}$$

in the HPC and

$$\sigma(e^+e^- \to \gamma + \text{invisible particles}) = (6.0 \pm 1.9) \text{ pb}$$

in the FEMC. The error quoted is statistical only. Taking into account errors on the background, on the detection efficiencies and on the event selection procedure, the systematic error is 0.7 pb in the HPC acceptance and 0.6 pb in the FEMC acceptance. In the case of the HPC the systematic error is dominated by the knowledge of the trigger efficiency and the event selection procedure. In the case of the FEMC the error comes mainly from the accuracy with which one can define the edge of the veto cone used to suppress the QED background.

3.1 Number of neutrinos

All the selected events were used to measure the cross-section of the reaction $e^+e^- \to \nu\bar{\nu}\gamma$. The cross-section of this process inside the acceptance of the detectors was computed by Monte Carlo simulation [1] as a function of the number of neutrino generations. The

result is shown in figure 2. From this plot, using the measured cross-sections, the number of neutrinos was determined to be

$$N_\nu = 3.1 \pm 0.6 \pm 0.1$$

averaging the independent measurements in the HPC and FEMC acceptances. The first error is the combination of the statistical and of the uncorrelated systematic errors, the second is the common systematic error. This value is in agreement with the number of neutrinos measured with the same method at LEP I [7,8].

3.2 Trilinear gauge boson couplings

The process $e^+e^- \to \nu\bar{\nu}\gamma$ can probe anomalous coupling in the $ZV\gamma$ vertex, where $V = Z$ or γ. The observation of such a coupling would be an indication of new physics, since the SM predicts a rate too small to be observed in current data or in data anticipated from future experiments. A limit on the $ZZ\gamma$ vertex using single photon events was obtained at $\sqrt{s} = M_Z$ by the L3 experiment [9]. At $\sqrt{s} = 130$ to 136 GeV the small integrated luminosity results in a weaker limit on $ZZ\gamma$ coupling, but it allows the study of the $Z\gamma\gamma$ vertex. A $WW\gamma$ three boson coupling contribution also arises in $\nu\bar{\nu}\gamma$ production from photon radiation from the exchanged W, but it is so small ($\ll 1\%$) at these energies that it may be neglected.

Following the study made in [10] on the non-Standard Model γZ production, the anomalous coupling can be described by four form factors, h_i^V (with i =1,2,3,4), whose dependence on the energy scale is parametrised as

$$h_i^V = h_{i0}^V/(1 + s/\Lambda^2)^n$$

where h_{i0}^V is the limit value of the coupling for $s = 0$, Λ is the energy scale at which a novel interaction would become manifest, and n=3,4 have been assumed for $h_{1,3}^V$ and for $h_{2,4}^V$ respectively.

The kinematic region sensitive to an anomalous coupling is that with high photon energies and large photon polar angles. Only the 10 events in the barrel and with $E_\gamma >$ 25 GeV were therefore considered. The only contribution to the 10 events from the SM is the process $e^+e^- \to \nu\bar{\nu}\gamma$ and there is no significant source of background.

Comparing the cross section in this kinematic region with the cross section of reference [10] allows 95% C.L. limits to be obtained as shown in Figure 3 for the two correlated parameters h_3^γ and h_4^γ, assuming all the others equal to zero. The same contour is obtained for h_1^γ,h_2^γ. The projected 95% C.L. limits are:

$$|h_{1,3}^\gamma| < 3.8 \qquad \text{and} \qquad |h_{2,4}^\gamma| < 9.1$$

at a scale $\Lambda = 500$ GeV. While the latter is still too large to be meaningful, the former is close to the limits set by the Tevatron experiments [11].

3.3 Limits on compositeness

Compositeness models predict several new particles which do not exist in the Standard Model. A specific Preon Model, studied in [12], is considered in this letter. It predicts several new particles, some of which contribute to the cross-section of process (1). In particular it predicts the existence of a W-like particle, U, and a new neutral boson D, which can mediate in the production of a pair of weakly interacting (ν-like) particles $l_S\bar{l}_S$

through the t-channel process $e^+e^- \to \gamma l_S \bar{l_S}$ and the s-channel process $e^+e^- \to D \to \gamma l_S \bar{l_S}$. The neutral state U^o can be produced by the exchange of D or Z (see figure 4).

Calculating the cross-sections in the hypothesis that a new boson D exists with $M_D = 5M_Z$ and summing the contributions to the cross-sections coming from direct production of $U^\circ \bar{U}^\circ$ pairs and exchange of $U^\pm$, a limit can be obtained on M_U from the measured $\sigma(e^+e^- \to \gamma +$ invisible particles) after subtracting the contribution expected from the production of three neutrinos in the Standard Model. The limit shown in figure 4 is

$$M_U > 43 \text{ GeV}/c^2 \quad \text{at } 95\% \text{ C.L.}$$

In the near future LEP200 will provide a good test of this model, since it predicts observable cross-sections in the region $\sqrt{s} = 150 - 200$ GeV for M_U in the range 50 - 60 GeV.

3.4 Limits on production of unknown neutral states

The data collected allow the search for a new particle, X, produced in association with a photon in the reaction $e^+e^- \to \gamma$X. If X is undetectable or decays invisibly, then it could be produced in the single photon topology.

The limit is calculated from the recoil mass distribution, assuming that the width of the X particle (including resolution) is less than 2 GeV and taking into account the expected background. The upper limit at the 95% confidence level of the cross-section for $e^+e^- \to \gamma$X, with the photon produced in the angular region $45^\circ < \theta_\gamma < 135^\circ$, is shown in figure 5.

Notice that previous limits set at lower centre-of-mass energies [8] are slightly improved in the region around 90 GeV.

4 Conclusions

With the 5.83 pb^{-1} of data collected at the centre of mass energy of 130 and 136 GeV reached by LEP in autumn 1995, a study of the production of single photon in the final state with no other interacting particle in the DELPHI detector has been performed. The Standard Model contribution from $e^+e^- \to \nu\bar{\nu}\gamma$ yields the measurement of the number of neutrino generations of $N_\nu = 3.1 \pm 0.6 \pm 0.1$. No excess of events has been observed, and limits have been set on possible new physics.

Acknowledgements

We are grateful to U. Baur, B. Mele, H. Czyz, O. Nicrosini and L. Trentadue for very useful discussions.
We are greatly indebted to our technical collaborators and to the funding agencies for their support in building and operating the DELPHI detector, and to the members of the CERN-SL Division for the excellent performance of the LEP collider.

References

[1] G. Montagna et al., Nucl. Phys. B452 (1996) 161.

[2] S. Ambrosanio and B. Mele, Phys. Rev. D52 (1995) 3900;
S. Ambrosanio et al., Universita di Roma "La Sapienza" HEP-PH 9601292.

[3] VENUS Coll., N.Hosoda et al.,Phys. Lett. B331 (1994) 211;
TOPAZ Coll., T.Abe et al.,Phys. Lett. B361 (1995) 199;
AMY Coll., Y.Sugimoto et al., submitted to Phys. Lett. B.

[4] DELPHI Coll., P. Abreu et al., CERN-PPE/95-194, submitted to Nucl. Instr. and Meth..

[5] D. Gillespie and T. Malmgren, DELPHI 94-46 CAL. 155.

[6] M. Caffo, R. Gatto and E. Remiddi, Phys. Lett. B173 (1986) 91;
M. Caffo, R. Gatto and E. Remiddi, Nucl. Phys. B286 (1987) 293.

[7] L3 Coll., O. Adriani et al., Phys. Lett. B292 (1992) 463;
ALEPH Coll., D. Buskulic et al., Phys. Lett. B313 (1993) 520;
OPAL Coll., M.Z. Akrawy et al, Zeit. Phys. C50 (1991) 373.

[8] R. Akers et al., OPAL Coll., Zeit. Phys. C65 (1995) 47;
P. Abreu et al., DELPHI Coll., CERN-PPE/96-03, submitted to Zeit. Phys. C.

[9] L3 Coll., F. Adeva et al., Phys. Lett. B346 (1995) 190.

[10] U. Baur and E. Berger, Phys. Rev. D47 (1993) 4889;
for modifications of the generator for e^+e^- collisions: U. Baur,private communication.

[11] CDF Coll., F. Abe et al., Phys. Rev. Lett. 74 (1995) 1941;
D0 Coll., S. Abachi et al., Phys. Rev. Lett. 75 (1995) 1034.

[12] H. Senju, Prog. Theor. Phys. 92 (1994) 611 and references therein;
H. Senju, Prog. Theor. Phys. 95 (1996) 455.

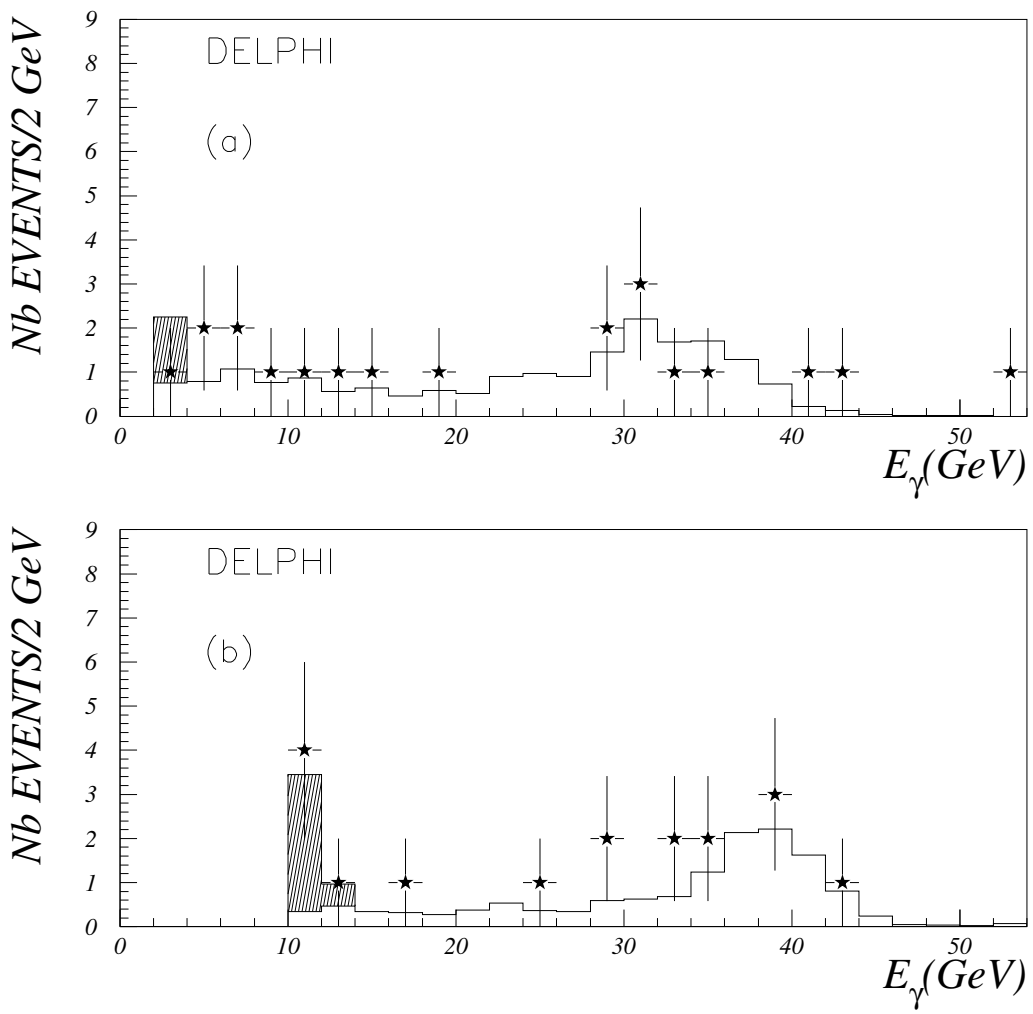

Figure 1: Energy spectrum of selected single photons a) in the barrel region (HPC) and b) in the forward region (FEMC). The hatched histogram is the background from the QED process $e^+e^- \to \gamma e^+e^-$, and the unhatched histogram is the expected spectrum from $e^+e^- \to \nu\bar{\nu}\gamma$. The event in (a) with E_γ=52. GeV is close to a crack of the detector and an α is mixed in its deposited energy, which is therefore badly determined.

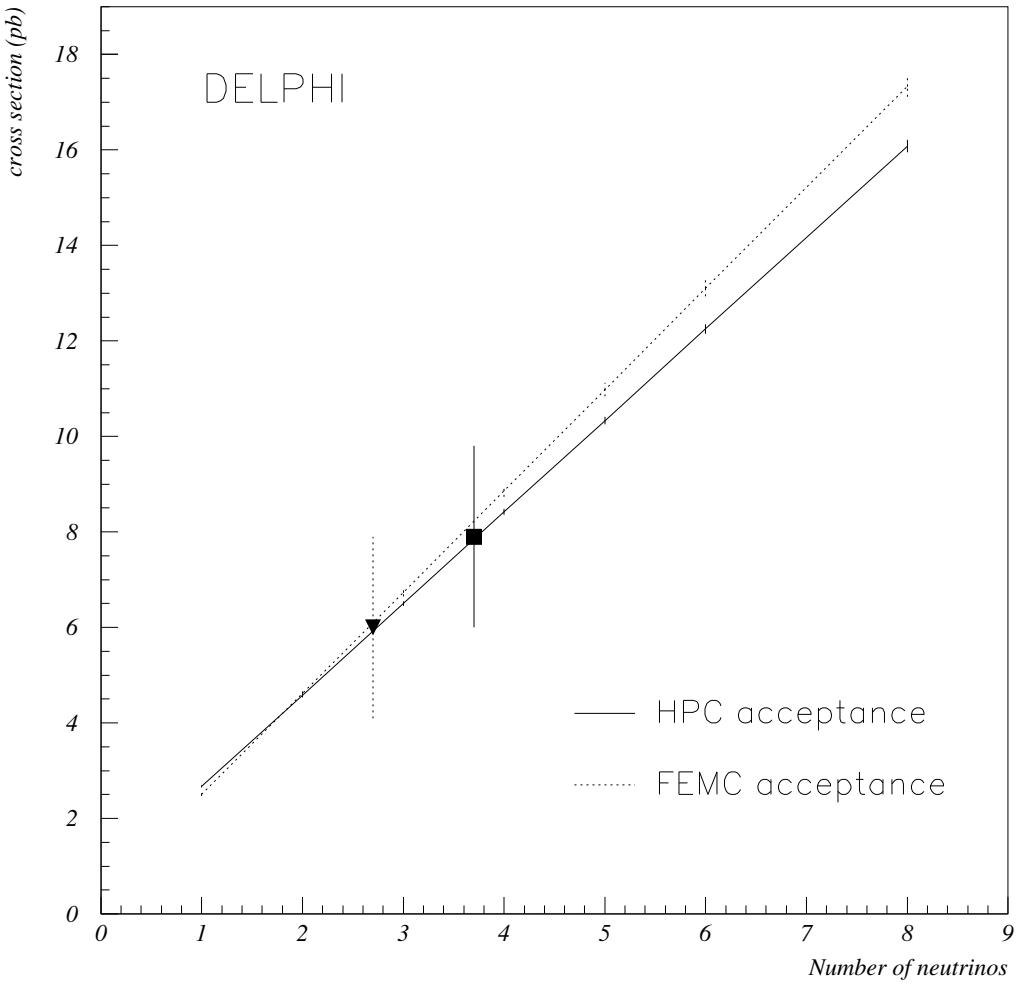

Figure 2: Cross-sections for radiative neutrino production in the region of acceptance of the HPC (square for the data and solid line for theoretical prediction) and FEMC (triangle and dotted line respectively).

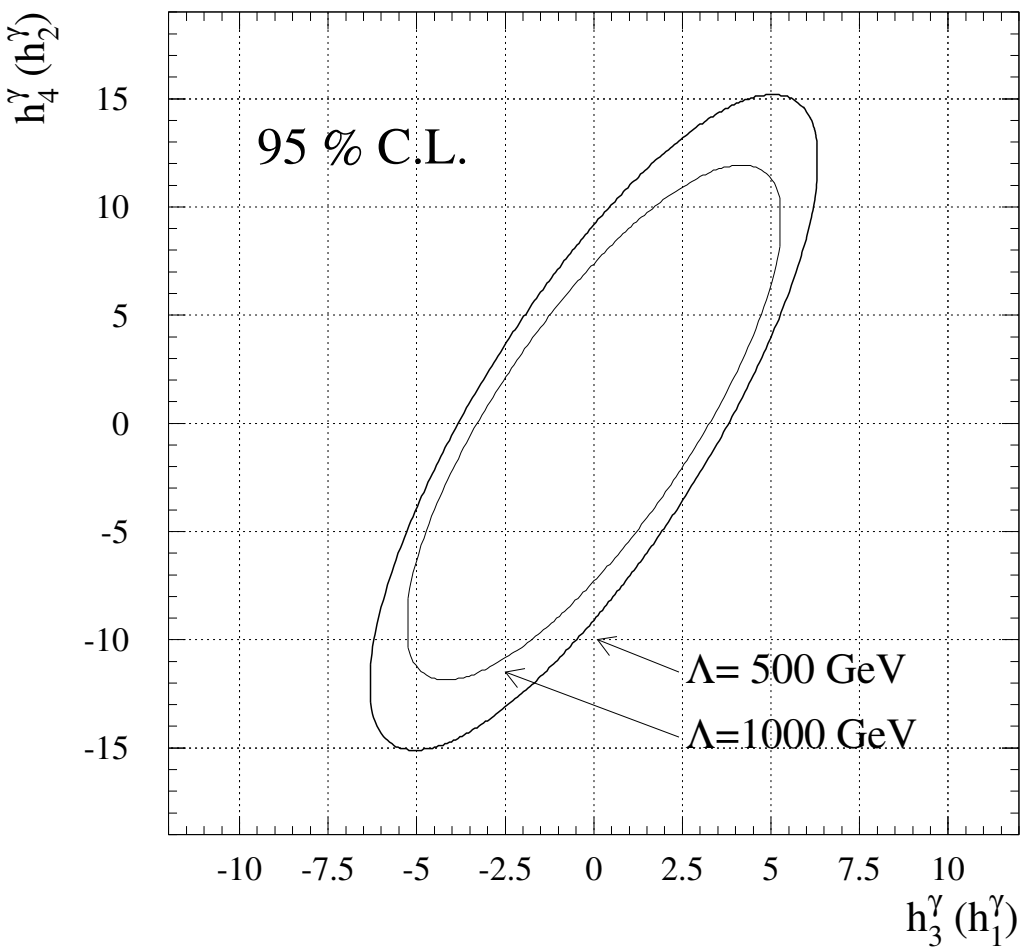

Figure 3: Upper limits at the 95% C.L. on the $Z\gamma\gamma$ coupling from the DELPHI single photon data for two different values of Λ.

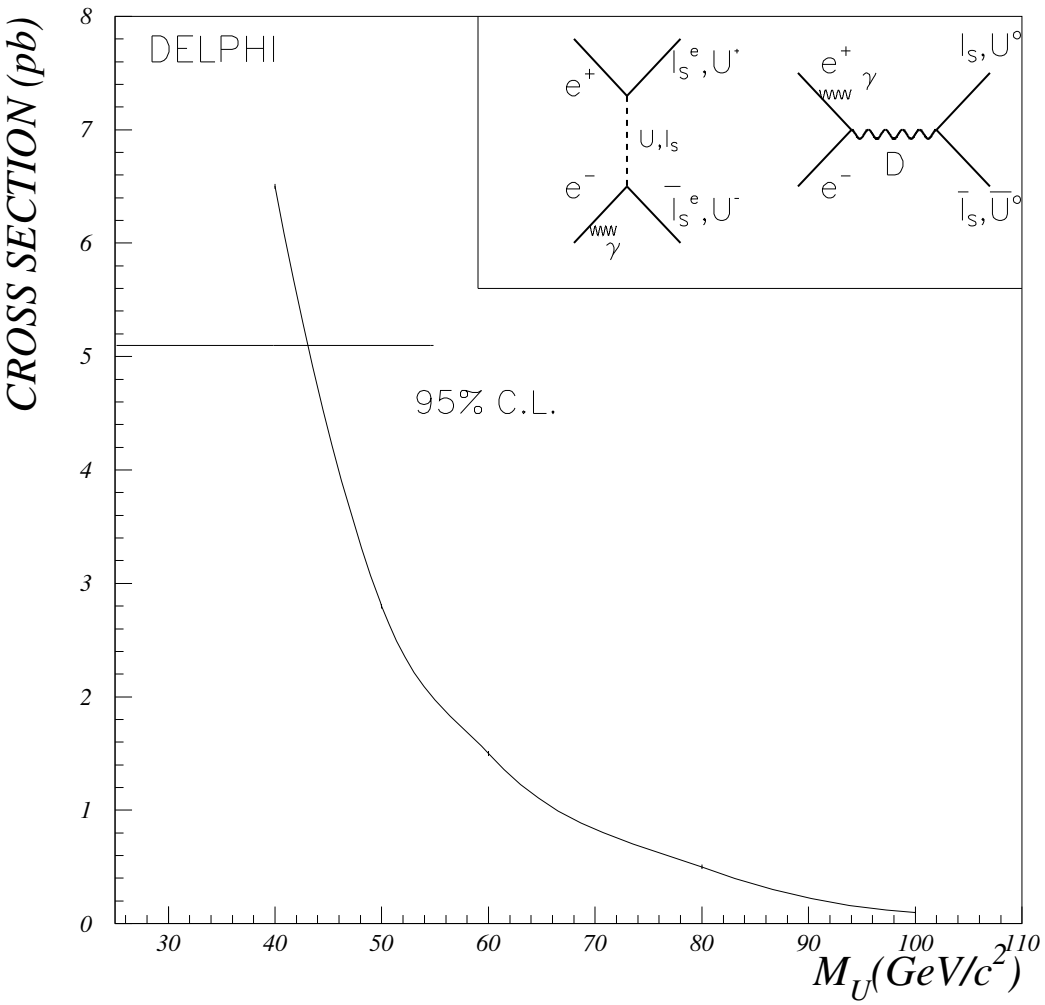

Figure 4: Limit at 95% C.L. for the mass of the W-type U boson. The curve shows the predicted cross section as a function of M_U according to [10]. The insert shows two examples of the Feynman graphs contributing to the calculated cross-sections.

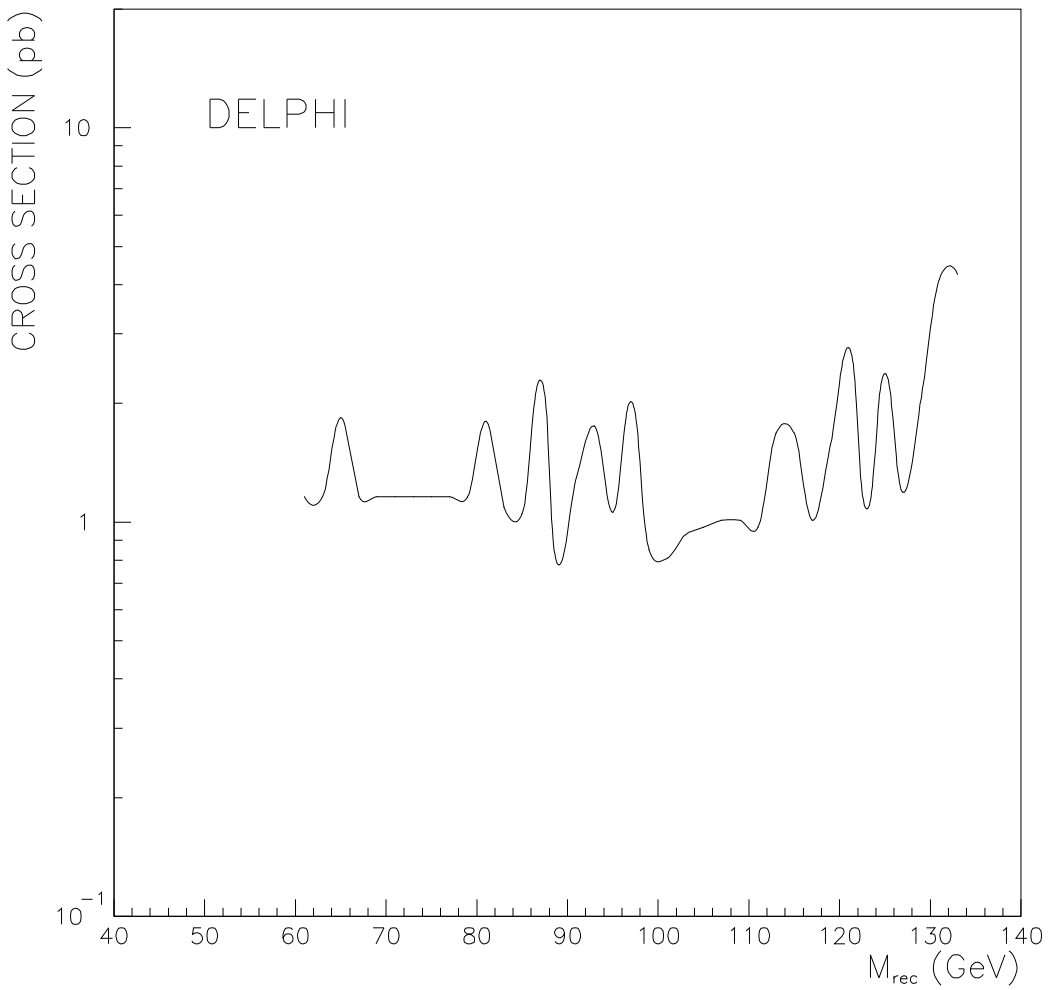

Figure 5: Upper limit at 95% C.L. for the cross-section of γX final state as a function of the mass of X.